



Woodhead, J., Truman, C. E., & Booker, J. D. (2015). Modelling of Dynamic Friction in the Cold Forming of Plain Spherical Bearings. In WIT Transactions on Engineering Sciences: Surface Effects and Contact Mechanics including Tribology XII. (Vol. 91). WIT Press, Southampton. 10.2495/SECM150131

Publisher's PDF, also known as Final Published Version

Link to published version (if available):  
[10.2495/SECM150131](https://doi.org/10.2495/SECM150131)

[Link to publication record in Explore Bristol Research](#)  
PDF-document

## University of Bristol - Explore Bristol Research

### General rights

This document is made available in accordance with publisher policies. Please cite only the published version using the reference above. Full terms of use are available:  
<http://www.bristol.ac.uk/pure/about/ebr-terms.html>

### Take down policy

Explore Bristol Research is a digital archive and the intention is that deposited content should not be removed. However, if you believe that this version of the work breaches copyright law please contact [open-access@bristol.ac.uk](mailto:open-access@bristol.ac.uk) and include the following information in your message:

- Your contact details
- Bibliographic details for the item, including a URL
- An outline of the nature of the complaint

On receipt of your message the Open Access Team will immediately investigate your claim, make an initial judgement of the validity of the claim and, where appropriate, withdraw the item in question from public view.

## **Modelling of dynamic friction in the cold forming of plain spherical bearings**

J. Woodhead, C. E. Truman & J. D. Booker

*Department of Solid Mechanics, University of Bristol, UK*

### **Abstract**

Nosing is a cold forming process used in the manufacture of plain spherical metal bearings. The process ensures the outer bearing race conforms to the shape of the inner race, with a composite liner in-between to provide a low frictional moment. These bearings need to be precision engineered to cope with the large forces and demanding environments they operate within, finding wide application in the aerospace industry. Increasingly, Finite Element (FE) analysis is used to predict complex material behaviour in cold forming processes to support industrial experience in developing products and determining associated process settings. On-going work in this area aims to provide industry with validated FE models across a range of bearing sizes, with measured stochastic data accounting for uncertainties in material properties, strain-rate sensitivity, friction and geometric parameters, to enhance model simulations and provide confidence in new bearing introductions where experimental trials are expensive and time-consuming. Ultimately, a costly and time-consuming experimental process can be replaced with a virtual rapid one, in order to mitigate defects and minimise failure rates in production.

In this paper, a repeatable method for determining a pressure versus friction relationship is outlined using traditional ring compression testing combined with friction calibration charts, determined via FE simulation, for a range of different materials. This paper builds upon previously published work on modelling the nosing process with strain-rate sensitive data. Calculations will be validated against stochastic experimental data to ensure the developed methods are robust.

*Keywords: friction, cold forming, nosing, modelling, FEA.*



# 1 Introduction

## 1.1 Nosing

Nosing, otherwise known as ‘tube-end forming’, is a cold-metal forming process used in the manufacture of plain spherical bearings [1], to which there are three main components; a central inner race (ball) enables the bearing to be axially supported; an outer race (sleeve) provides a platform for other components in the assembly; and a composite material (liner) in between, affixed to the latter with adhesive, provides lubrication and frictional properties during operation (Figure 1). Applications are wide and varied including, but not limited to, bearings for fixed/rotary-wing pitch control, dampers, the main central and tail rotary shafts, flap controls, cargo bay doors and under carriages [2]. In the nosing process the sleeve is placed, together with the ball and liner, in between two spherical dies (Figure 1(a)). The upper die displaces along the natural axis, and the bearing is subject to compression at the contact interface between the die and the sleeve, as the force is translated axially. This causes the sleeve to undergo elastic-plastic deformation, until it geometrically conforms to the shape of the ball (Figure 1(b)).

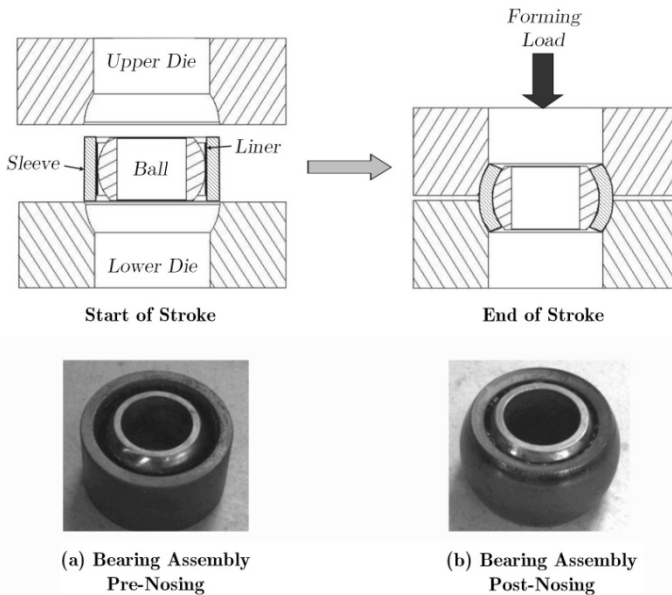


Figure 1: Schematic of the nosing operation.

## 1.2 Coefficient of friction

Tribology is a broad field incorporating surface contact, wear, lubrication and ultimately the effect of friction on these interactions. A tribological system can

be extremely complex, even between just a pair of surfaces [3]. Friction is the resistance to that sliding interaction between surfaces in contact, under a normal load, and this impedance to the free movement at the interfaces affects the flow and deformation of the material, and hence the stresses placed into it. As the tool stresses are quite high in cold-forming processes (comparably with higher temperature processes), consequently the prediction of stresses is important, particularly for part/die geometry, energy consumption, defining tolerances and surface finishes, and press selection [3]. The applied forming load, strain distribution, tool and die life, surface quality and ultimately the stresses placed into the component during this process are all affected by the interaction between the surfaces in contact [4]; therefore, interpreting the correct value for the coefficient of friction is paramount. Due to the combination and quantity of variables continuously interacting which can influence a system, friction is inherently difficult to quantify even within a static problem. As such, a single 'global' value of friction is invariably specified for the modelling of dynamic problems [5]. Additionally, it is common to take these empirically-obtained values directly from classical texts, perhaps as experimentation can be costly and time-consuming.

Two models are generally used to represent friction in forming operations, namely Coulomb's Law (Equation 1) and the Law of constant (or Tresca) friction (Equation 2).

$$\tau_f = \mu\tau_n \quad (1)$$

whereby the coefficient of friction is  $0 \leq \mu \leq 0.577$ ,  $\tau_f$  is the friction stress,  $\tau_n$  is the normal contact pressure and  $\mu$  is the coefficient of friction.

$$\tau_f = mk \quad (2)$$

whereby the friction factor is  $0 \leq m \leq 1$ ,  $\tau_f$  is the friction stress,  $k$  is the shear stress and  $m$  is the friction factor.

Kobayashi *et al.* [3] state that Coulomb's Law adequately represents friction in sheet-metal forming operations, and that Tresca's Law is suitable for bulk forming deformation; however, Coulomb's Law is utilised within Abaqus CAE and is hence used in this analysis. Both can be determined by a ring test, whereby a flat ring of known material properties is compressed. The percentage change in internal diameter can then be compared to pre-calibrated charts to determine the friction conditions. Even though Kunogi [6] first suggested this method in 1956, Male and Cockcroft [7] were the first to improve the method. Subsequently, the ring compression test has gained wide acceptance, especially for processes involving bulk deformation [9]. However, to date, there is no universally-endorsed standard, yet there have been publications on this test by organisations such as ASTM [19].

### 1.3 Limitations of analytical/virtual models

Various analytical models, both theoretical and empirically informed, which attempt to describe the plastic deformation of cylinders, have been previously explored [10]. Of the analytical methods explored, few attempt to account for friction, via incorporating a variable for the coefficient of friction [8]. However, even these methods can fail to accurately predict the shape of the flow curve and magnitude of the forming load. The issue with this type of approach is that the model cannot dynamically change the coefficient of friction. For example, the friction can change due to a variation in lubrication, pressure, geometry, material etc. A 3d simulation of the nosing operation for a high-yield production bearing was created using Abaqus, and run for coefficients of friction ranging from  $0.05\mu$  to  $0.45\mu$ . The forming load was extracted from the results and plotted against the displacement for both dies, and the curve of best fit from the statistically-analysed experimental results obtained from the press were superimposed (Figure 2). It can clearly be seen how, according to the FE simulations, the coefficient of friction does change throughout the process, varying between friction coefficients of  $0.45\mu$  at the beginning of the process, and then decreasing to  $0.1\mu$  before finally increasing to  $0.15\mu$  at the end.

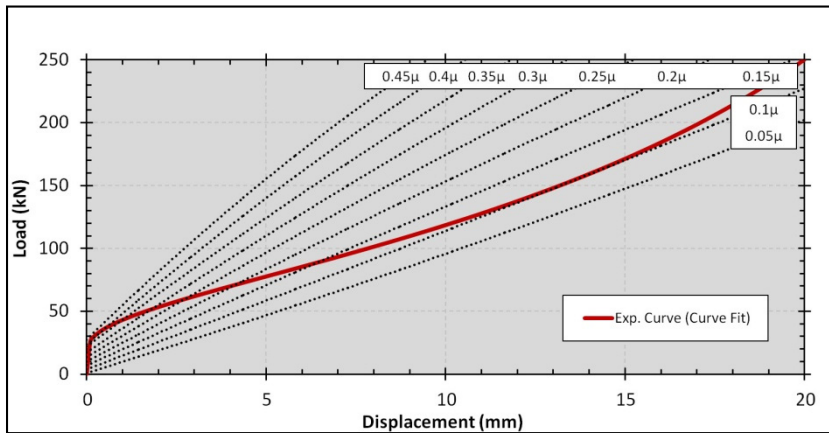


Figure 2: Effect of friction coefficient,  $\mu$ , on a load-displacement graph for the nosing process, with experimental 'steady-state' forming data.

Booker and Truman [11] indicate that, generally, the coefficient of friction reduces with increased pressure. This theory correlates with work by Tang and Kobayashi [12], and Cora *et al.* [4], and enforces the fact that a variable, or non-linear coefficient of friction is required to accurately predict load history of the nosing process. Failure to predict load history during product development can lead to any number of failure modes highlighted in Figure 3, resulting in extensive re-working or scrapping of the bearing altogether.

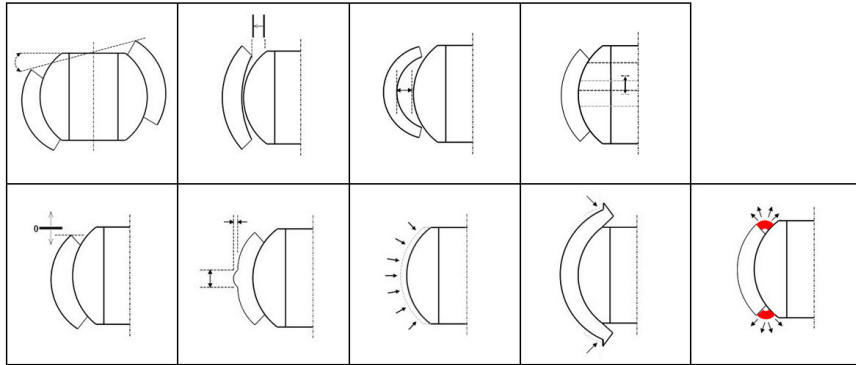


Figure 3: Nosing failure modes, from left to right; top row: tipping, open-mouth, church-window, liner slippage; bottom row: offset, Saturnisation, ball crushing, necking, adhesive bleed-out.

## 2 Methodology

### 2.1 Theory

In 1965, Male and Cockcroft [7] published a standard method for determining the coefficient of friction,  $\mu$ , using ring compression tests, although their work was based upon initial findings by Kunogi in 1956 [6]. A ring is compressed axially in between two flat platens, and the ring undergoes elastic-plastic deformation. The initial and final geometry is measured and compared to friction calibration curves (FCCs). If zero friction is present at the contact interface between the platens and ring surface (isotropy of the material, perfectly plastic and homogenous deformation are all assumed), the inner diameter of the ring will expand together with the outer diameter and maintain a constant width. The amount of friction affects the relationship between the geometric change in shape and the amount of deformation. This is because a degree of sticking occurs when friction is introduced, and hence the higher the friction, the slower the rate of expansion of the outer diameter of the ring, and once  $\mu$  reaches a critical value it becomes more energetically favourable for the material to flow inwards, and as such, the inner diameter reduces [7]. This method separates the geometric change produced by plastic deformation, from the mechanical properties of the sample material, therefore; the flow stress of the material need not be determined; only the initial and final dimensions of the sample are required.

### 2.2 Specimens

There is no consensus on the most suitable specimen size, however; theoretical studies [14, 15] indicate that maximum accuracy can be obtained if the ring geometry has a large internal diameter. If the internal diameter is too large

however, the ring may become unstable and buckle during deformation, although this effect can be mitigated by having a sufficiently shallow height [7]. This may be considered an issue when testing at elevated temperatures, because a smaller sample will result in greater heat-loss [6]; however, this is irrelevant to testing at cold temperatures. The most commonly used ratio of outer diameter to inner diameter to height (OD:ID:H) is 6:3:2 [15]; therefore, the following specimen was selected (Figure 4).

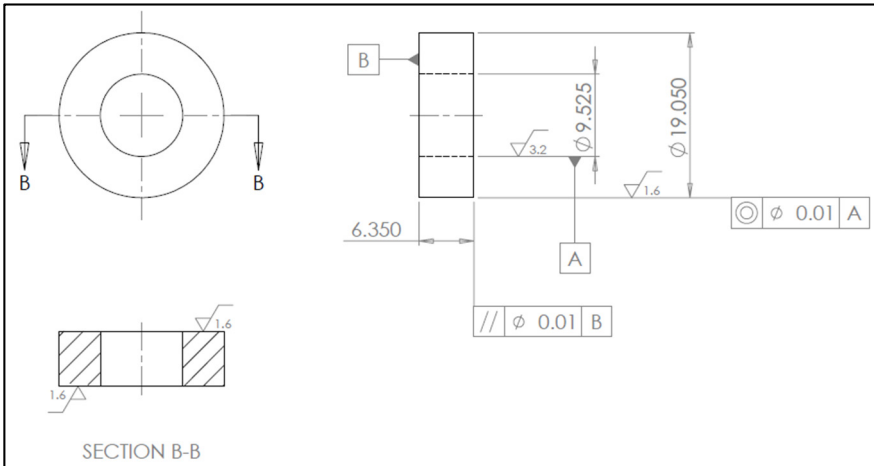


Figure 4: Engineering drawing of ring test specimens.

A total of 72 specimens were tested, 3 materials (212M36, AMS5643 and S80), 24 specimens of each material, 4 specimens at each deformation level. This ensured a sufficient number of specimens were tested in order that valid averages could be obtained, and also controlled the test specimens to a number which could be feasibly tested during the time. Consistent with the lubrication process used in production, Molykote lubricant was applied to all contact surfaces to ensure hydrodynamic lubrication between the platens and the extreme surfaces of the specimens, and promote uniform deformation throughout (i.e. no barrelling is desirable).

### 2.3 Testing parameters

There are no published documents relating to the testing and calibration of friction to date, and as alluded earlier there is also no internationally or nationally agreed methodology for the ring compression test. However, ASTM International standards stipulate criteria which must be conformed to for uniaxial compressive material testing [14], and testing henceforth adhered these standards. The height of the samples were reduced incrementally between 10 and 70% in intervals of approximately 10% (Figure 5), to ensure the pressure range required for modelling was achieved. The testing environment was room temperature (i.e. 20°C or 293.16K).

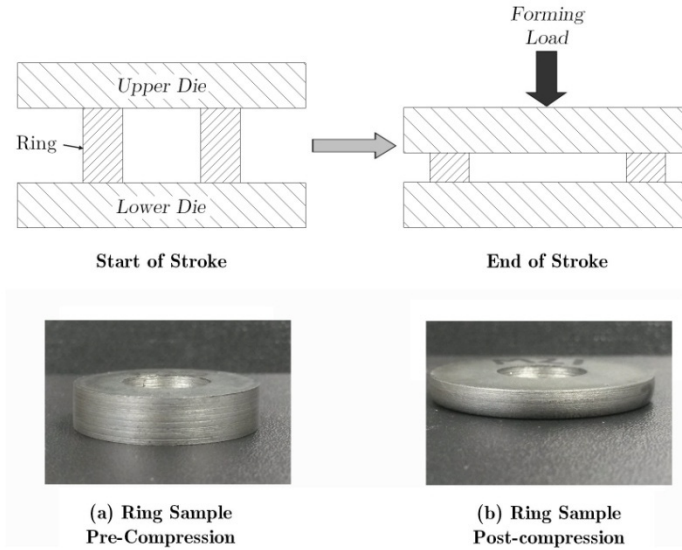


Figure 5: Schematic of the ring test.

## 2.4 Equipment and measurements

This test was performed on a four column press machine (Figure 6), manufactured by a reputable company, ensuring that the platens are brought down completely parallel to the specimen. The internal diameter of the specimens may take a non-circular shape after deformation, especially if there is any degree of anisotropy. Care was therefore taken to measure the internal diameter, which was achieved using an internal micrometer, taking a number of measurements to obtain an average.



Figure 6: Four-column press.



### 2.5 Friction calibration curves (FCCs)

Once a percentage reduction in inner diameter of the ring has been measured, a graph against the percentage reduction in height can be plotted and compared to published FCCs. There are various FCCs available, including Male and Cockcroft’s [7], established via experimental methods; Lee and Altan’s [16] as well as Liu’s [17], which took into account the effect of barrelling; Danckert and Wanheim’s [18], which took into account strain-hardening. Differences in these FCCs can be observed, which are the result of employing different friction models, ring geometry, together with the effects of barrelling and strain-hardening [19]. The generic published FCCs are not recommended to be used, because of these sample and test-specific variations [25, 26]; therefore, similar to authors such as Alves *et al.* [22], in this study the FCCs were obtained via FEM using Simulia’s Abaqus software.

### 3 Analysis

The following FCCs in Figure 7 show experimental results for material 212M36 alloy steel, together with curves fitted from FE-extracted data for friction coefficients ranging from  $0\mu$  to  $0.5\mu$ . The data was interpolated across the FCCs at each experimental data point to predict the coefficient of friction. The stress was calculated at each experimental data point as the load and final area of the samples is known. It is feasible to obtain a coefficient of friction of much greater magnitude (i.e. a rubber tire on a dry surface); however, mathematically speaking in terms of deformation mechanics, if Von Mises yield criterion is assumed, then a material yields at a maximum shear yield stress of

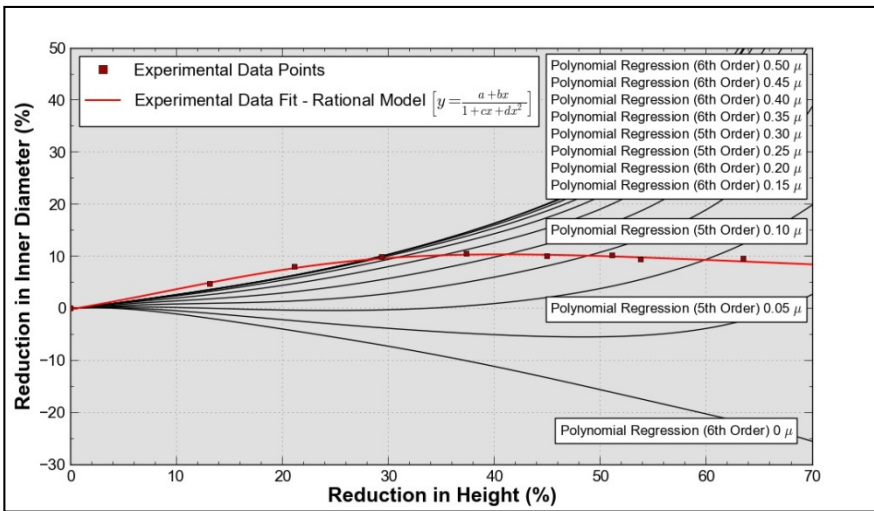


Figure 7: FCCs for 212M36 alloy steel.



approximately 0.5 times the normal stress. As the tangential (frictional) stress,  $\tau_f$ , increases it will eventually equal the shear yield strength,  $k$ , of the material. The normal force may increase further, however, because the frictional shear force remains constant, the coefficient of friction decreases due to the application of Coulomb's Law [4, 5]. Therefore, an upper limit of  $0.577\mu$  is invariably assumed when using Coulomb's Law. Even though the data initially displays a friction coefficient of greater magnitude (Figure 7), this upper-bound limit has been applied to these experimental results, and a graph of pressure against friction can be plotted for all three materials (Figure 8).

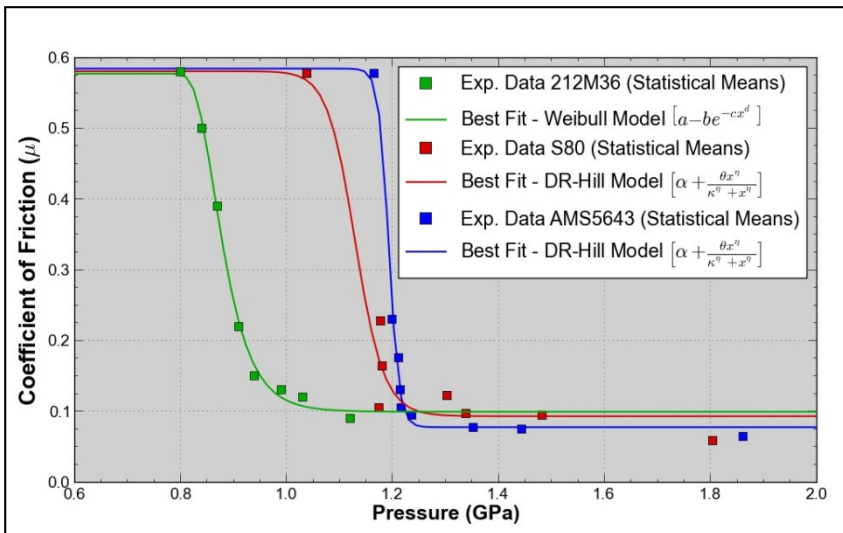


Figure 8: Variation in coefficient of friction with change in pressure for 212M36, S80 and AMS5643 alloy steels.

#### 4 Friction-dependent FE

Details of the virtual model, including part/material/mesh properties and boundary conditions are covered in a previous paper [10]. The load history results from Abaqus, for a high-yield production bearing, can be seen in Figure 9, which compares forming load data collected from the production environment, with three FE models generated in Abaqus; namely, a non-strain-rate dependent model with a static global coefficient of friction; a strain-rate dependent model with a static global coefficient of friction; and a strain-rate dependent model with a dynamic coefficient of friction.

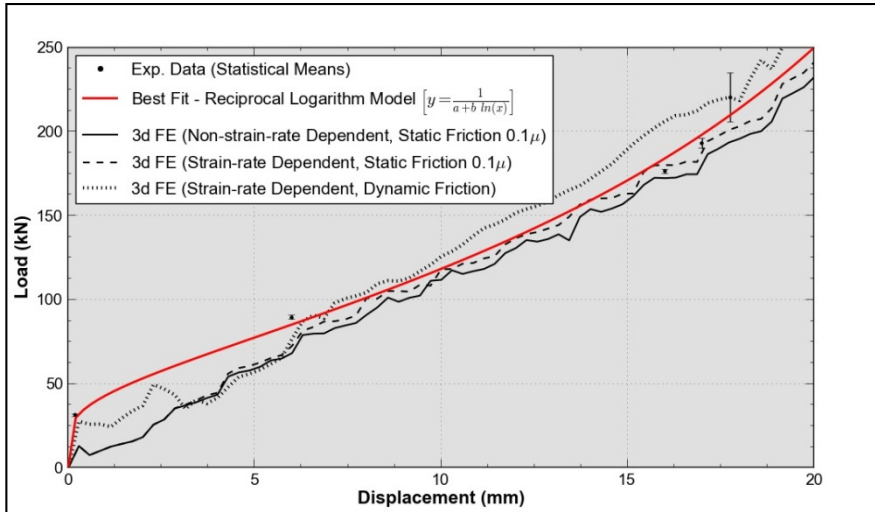


Figure 9: A statistically analysed steady-state load-history of a high-yield production bearing, with virtual FE models

## 5 Conclusions

Friction is sometimes neglected or simplified in industrial practice, perhaps due to the complex nature of a tribological system and the amount of variables that need to be considered. Another contributing factor may be that the cost of lubrication and special coatings to reduce friction, comparably with the cost of raw material, equipment and labour required to investigate, is small [24]; therefore, the incentive to research this phenomenon and/or change industrial practices is low. However, with specific reference to cold forming, one of the largest factors contributing to lost production is excess die wear, and failure whereby friction is the leading contributing factor [24], highlighting the importance of understanding this area. This work shows that the coefficient of friction does decrease with increasing pressure, from 0.577 to 0.091 for alloy Steel 212M36, 0.064 for alloy Steel AMS5643, and 0.058 for alloy Steel S80; at maximum pressure; however, this phenomenon is not fully understood, indicating that there may be more realistic empirical relationships to express friction at the interface of two surfaces. A repeatable, statistical, method to evaluate the change in friction with pressure is outlined, from which the following may be implemented:

- A friction-pressure relationship whereby the friction can be determined at any value of pressure;
- A more suitable value of static friction for the working conditions within a process, which can be used in analytical equations;
- A dynamic friction model to improve the overall shape of FE load-displacement curves for the nosing process;

- A reduction in percentage error in determining the final forming load at maximum displacement from 13.8% and 9.6% (for the static friction models), to 0.1% (for the dynamic friction model).

Future emphasis is placed on a frequently recommended, but rarely implemented, dynamic-friction finite-element model [7, 8], and will entail incorporating this non-linear, strain-rate dependent material behaviour, and dynamic friction, into existing FE models to reduce the percentage error within load history predictions of a range of bearing sizes.

## References

- [1] A. Orsolini and J. D. Booker, "Modelling Capabilities Required for the Double Nosing Process in the Assembly of Spherical Plain Bearings," in *Proceedings of the Institution of Mechanical Engineers, Part B: Journal of Engineering Manufacture*, 2012, pp. 226–930.
- [2] J. J. C. Hoo and W. B. Green, *Bearing Steels: Into the 21st Century*, Illustrate., no. 1327. ASTM International, 1998, p. 524.
- [3] S. Kobayashi, T. Altan, and S.-I. Oh, *Metal Forming and the Finite-Element Method*, 4th Edition. Oxford: Oxford University Press, 1989, p. 391.
- [4] Ö. N. Cora, M. Akkök, and H. Darendeliler, "Modelling of Variable Friction in Cold Forging," *Proc. Inst. Mech. Eng. Part J J. Eng. Tribol.*, vol. 222, no. 7, pp. 899–908, 2008.
- [5] Y. Lu, "Study of Preform and Loading Rate in the Tube Nosing Process by Spherical Die," *J. Comput. Methods Appl. Mech. Eng.*, vol. 194, pp. 2839–2858, 2005.
- [6] M. Kunogi, "A New Method of Cold Extrusion," *J. Sci. Res. Institute, Tokyo*, vol. 50, no. 1437, pp. 215–246, 1956.
- [7] A. T. Male and M. G. Cockcroft, "A Method for the Determination of the Coefficient of Friction of Metals Under Conditions of Bulk Plastic Deformation," *Inst. Met.*, vol. 93, no. 3, pp. 38–46, May 1965.
- [8] S. Kalpakjian and S. R. Schmid, *Manufacturing Processes for Engineering Materials*, Third. Pearson Education, 2003, p. 954.
- [9] R. G. Narayanan, M. R. Mitchell, R. E. Link, M. Gopal, and A. Rajadurai, "Influence of Friction in Simple Upsetting and Prediction of Hardness Distribution in a Cold Forged Product," *J. Test. Eval.*, vol. 36, no. 4, pp. 1–13, 2008.
- [10] J. Woodhead and J. D. Booker, "Modelling of Nosing for the Assembly of Aerospace Bearings," *Exp. Appl. Mech.*, vol. 4, pp. 327–337, 2013.
- [11] J. D. Booker and C. E. Truman, "A Statistical Study of the Coefficient of Friction under Different Loading Regimes," *J. Phys. D. Appl. Phys.*, vol. 41, no. 17, pp. 1–12, 2008.
- [12] M. Tang and S. Kobayashi, "An Investigation of the Shell Nosing Process by the Finite-Element Method. Part 1: Nosing at Room Temperature (Cold Nosing)," *J. Eng. Ind.*, vol. 104, no. 82, pp. 305–311, 1982.



- [13] M. Kunogi, "On Plastic Deformation of Hollow Cylinders under Axial Compressive Loading," *J. Sci. Res. Institute, Tokyo*, vol. 50, no. 30, pp. 215–246, 1954.
- [14] H. Kudo, "An Analysis of Plastic Compressive Deformation of Lamella between Rough Plates by Energy Method," in *Proceedings of the 5th Japan National Congress for Applied Mechanics*, 1955, p. 295.
- [15] H. Sofuoglu and H. Gedikli, "Determination of Friction Coefficient Encountered in Large Deformation Processes," *Tribol. Int.*, vol. 35, pp. 27–34, 2002.
- [16] C. H. Lee and T. Altan, "Influence of Flow Stress and Friction Upon Metal Flow in Upset Forging of Rings and Cylinders," *J. Eng. Ind.*, vol. 94, no. 3, pp. 775–782, Aug. 1972.
- [17] J. Y. Liu, "An Analysis of Deformation Characteristics and Interfacial Friction Conditions in Simple Upsetting of Rings," *J. Eng. Ind.*, vol. 94, no. 4, pp. 1149–1155, Nov. 1972.
- [18] J. Danckert and T. Wanheim, "Analysis of the Ring Test Method for the Evaluation of Frictional Stresses in Bulk Metal Forming Processes," *CIRP Ann. – Manuf. Technol.*, vol. 37, no. 1, pp. 217–220, 1988.
- [19] V. Mandic and M. Stefanovic, "Friction Studies Utilizing the Ring – Compression Test – Part I," in *8th International Tribology Conference*, 2003, pp. 44–51.
- [20] K. P. Rao and K. Sivaram, "A Review of Ring-compression Testing and Applicability of the Calibration Curves," *J. Mater. Process. Technol.*, vol. 37, pp. 295–318, 1993.
- [21] H. Sofuoglu and J. Rasty, "On the Measurement of Friction Coefficient Utilizing the Ring Compression Test," *Tribol. Int.*, vol. 32, no. 6, pp. 327–335, 1999.
- [22] M. L. Alves, P. A. F. Martins, and J. M. C. Rodrigues, "Simulation of Three-dimensional Bulk Forming Processes by Finite Element Flow Formulation," *J. Model. Simul. Mater. Sci. Eng.*, vol. 11, pp. 803–821, 2003.
- [23] T. Altan, G. Ngaile, and G. Shen, *Cold and Hot Forging: Fundamentals and Applications*. ASM International, 2005, p. 342.
- [24] A. Buschhausen, K. Weinmann, T. Altan, and J. Lee, "Evaluation of Lubrication and Friction in Cold Forging using a Double Backward-Extrusion Process," *J. Mater. Process. Technol.*, vol. 33, no. 1–2, pp. 95–108, August 1992.
- [25] M. Gierzyńska-Dolna and P. Lacki, "Some Aspects of Modelling of Metal Forming Processes," *Comput. & Struct.*, vol. 81, no. 8–11, pp. 605–613, 2003.
- [26] X. Lai, Y. Xia, X. Wu, and Q. Zhou, "An Experimental Method for Characterizing Friction Properties of Sheet Metal under High Contact Pressure," *Wear*, vol. 289, pp. 82–94, June 2012.

